

Use of the Surface Forces Apparatus to Directly Measure the Influence of Self-Assembled Monolayers on the Adhesion and Deformation of Rough Solids

R. A. Quon,[†] A. Ulman,[‡] and T. K. Vanderlick*

Department of Chemical Engineering, University of Pennsylvania, Philadelphia, Pennsylvania 19104, Department of Chemistry, Chemical Engineering and Materials Science, Polytechnic University, Brooklyn, New York 11201, and Department of Chemical Engineering, Princeton University, Princeton, New Jersey 08544

Received June 2, 1999. In Final Form: January 6, 2000

A contact mechanics approach is used to study the role of model sub-boundary lubricants on the deformation and adhesion between rough solids. Self-assembled monolayers of *n*-octadecanethiol and 1-hydroxylunicosanethiol adsorbed to microscopically rough gold are brought into contact with molecularly smooth mica using a surface forces apparatus. Deformations at the interface and concurrently those in the bulk were measured while controlling applied loads. The effect of the SAMs is deduced by comparing the behavior of these systems to that of uncoated gold as previously put forward. Most significantly, the presence of a self-assembled monolayer sharply defines the strength of adhesion as measured by precise pull-off forces for given loading conditions. As compared to uncoated gold, the coated gold also exhibits a lesser amount of microdeformation under equivalent loading. Moreover the microdeformations are reversible upon relief of the load. This elastic regime is used to estimate the compressibility of each self-assembled monolayer. While the deformations at the interface are recoverable, deformations of the bulk are not. The hysteresis of the bulk is attributed to the monolayer; the more adherent system of 1-hydroxylunicosanethiol and mica exhibits greater hysteresis than contact between *n*-octadecanethiol and mica.

Introduction

The chemical and mechanical properties of microscopically thin boundary layer films are known to dramatically affect macroscopically measured phenomena such as adhesion and friction.¹ Particular interest lies in sub-boundary lubricants—films which bind strongly to a substrate to form a uniform layer, such as Langmuir–Blodgett layers or self-assembled monolayers.² Understanding the behavior of thin overlayer films in adhesion, friction, and lubrication has significant technological motivation, ranging from the improvement of magnetic storage devices to the development of micromachines. Self-assembled monolayer (SAM) films^{3–6} are ideal for studying the influence of molecular boundary layers on contact between solids because of the ability to tailor the film structure and surface chemistry. Moreover, construction of monomolecular films via self-assembly offers an especially simple means of creating a well-defined surface.

Considerable experimental effort has been devoted to investigating the role of thin boundary layer films in adhesion.^{7–11} Though adhesion is understood to be predi-

cated on molecular attractions at an interface, experimental study between solids must consider contact mechanics. Pioneering work by Johnson, Kendall, and Roberts (JKR)¹² provided a theoretical and experimental framework for understanding contact, deformations, and adhesion between smooth, elastic bodies. Their work describes adhesion as a balance of applied loads with adhesive and elastic forces.

A substantial body of experimentation shows the JKR approach to be fairly descriptive of adhesive contact between smooth elastic solids.^{7,12,13} Surface irregularities, such as roughness, are even found to be inconsequential if the materials are compliant enough to form an intimate (i.e., molecular) interface.¹⁴

Adhesion hysteresis, however, is often observed in the presence of a sub-boundary lubricant, especially if the thin overlayer film is polymeric in nature.^{8–11,15,16} Unfortunately, the origin of this hysteresis depends critically on the nature of the experimental setup. Devices to examine this phenomenon in the framework of contact mechanics fall in two categories: the well-established surface forces apparatus¹⁷ and the so-called JKR machine.^{12,18}

* To whom correspondence should be addressed at Princeton University.

[†] University of Pennsylvania.

[‡] Polytechnic University.

(1) McFarlane, J. S.; Tabor, D. *Proc. R. Soc. London A* **1950**, *202*, 224.

(2) Stanley, H. M.; Etison, I.; Bogy, D. B. *J. Tribol.* **1990**, *112*, 98–104.

(3) Ulman, A. *An Introduction to Ultrathin Organic Films from Langmuir–Blodgett to Self-Assembly*; Academic Press: New York, 1991.

(4) Ulman, A. *Chem. Rev.* **1996**, *96*, 1553–1554.

(5) Nuzzo, R. G.; Zegarski, B. R.; Dubois, L. H. *J. Am. Chem. Soc.* **1987**, *109*, 733–740.

(6) Bain, C. D.; Whitesides, G. M. *Angew. Chem., Int. Ed. Engl.* **1989**, *28*, 506–512.

(7) Chaudhury, M. K.; Whitesides, G. M. *Langmuir* **1991**, *7*, 1013–1025.

(8) Chen, Y. L.; Helm, C. A.; Israelachvili, J. N. *J. Phys. Chem.* **1991**, *95*, 10736–10747.

(9) Deruelle, M.; Leger, L.; Tirrell, M. *Macromolecules* **1995**, *28*, 7419–7428.

(10) Kim, S.; Choi, G. Y.; Ulman, A.; Fleischer, C. *Langmuir* **1997**, *13*, 6850–6856.

(11) Ruths, M.; Granick, S. *Langmuir* **1998**, *14*, 1804–1814.

(12) Johnson, K. L.; Kendall, K.; Roberts, A. D. *Proc. R. Soc. London A* **1971**, *324*, 301.

(13) Horn, R. G.; Israelachvili, J. N.; Pribac, F. *J. Colloid Interface Sci.* **1987**, *115*, 480–492.

(14) Fuller, K. N. G.; Tabor, D. *Proc. R. Soc. London A* **1975**, *345*, 327–342.

(15) Falsafi, A.; Deprez, P.; Bates, F. S.; Tirrell, M. *J. Rheol.* **1997**, *41*, 1349–1364.

(16) Chaudhury, M., K.; Owen, M., *J. Langmuir* **1993**, *9*, 29.

Investigations of adhesion and contact mechanics are well-suited to the surface forces apparatus (SFA), a device designed to measure the forces between, and associated deformations of, two curved surfaces in contact.¹⁷ Central to this force measuring technique is the use of multiple beam interferometry (MBI) to determine the separation between surfaces.¹⁹ This method, however, requires the construction of an interference filter from the experimental surfaces; mica is ideally suited for this purpose as it may be prepared molecularly smooth and uniformly thick. Thus, most studies using the SFA have been limited to studying the interactions between mica^{13,17,20,21} or between sufficiently smooth and compliant films which can be adsorbed to mica.^{11,8}

The prime advantage of the SFA technique is the ability to observe changes at the interface, as provided by interferometry. In addition, accompanying deformations of the bulk, as measured by changes of nominal area, can be concurrently measured. Chen et al.²² used the SFA to measure the compressibility of adsorbed surfactants and Langmuir–Blodgett films. Unfortunately, study of sub-boundary lubricants has been limited to those sets of molecules and films which readily bind or adsorb to mica. Furthermore, interactions between surfaces are usually limited to methylene chain interactions between surfactants, polymers, or combinations of the two.

The other device commonly used to study the effect of sub-boundary lubricants on the adherence of solids was developed in its current form by Maugis and Barquins, which we refer to as the JKR machine.¹⁸ Studies using this device^{9,10,23} consider contact involving at least one elastomeric solid; typically, an elastomeric spherical cap is brought into contact with a flat plate. The great advantage of this experimental setup is that interactions between solids other than mica may be considered, and consequently, a wider array of surfaces and sub-boundary lubricants can be investigated. Thin films of different chemical termination and film structure are grafted onto the spherical lens, or facing plate. Then, the two solids are contacted and changes in contact area with applied load are monitored. Often adhesion hysteresis is observed and is related to the chemical and mechanical properties of the film, as well as to the rate at which load is applied between the contacting bodies. Unfortunately, in these experiments the separation of viscoelastic bodies is not solely dictated by interactions at the interface. Energy is often dissipated within the bodies themselves, thus contributing to the ultimate work needed to separate the surfaces. Controversy still exists among practitioners of this approach as to the extent and source of apparent viscoelastic losses.^{9,24,25} Last, and most critically, this experimental method lacks the capability to directly observe any changes in deformations at the interface due to the presence of the thin overlayer films.

Another approach to learning more about adhesion and the role of sub-boundary lubricants blends the mechanical elegance of the SFA with the robust set of experimental systems available for study with the JKR machine.

Recently, Levins et al.^{26–29} demonstrated how metal surfaces such as gold and silver can be effectively studied by using the SFA. This advancement not only extends the variety of films available for study in the SFA but also permits investigations of the effect of nanometer-scale roughness on adhesion.³⁰ Quon et al.³¹ examined this effect for the case of gold metal films contacting mica and showed how deformations of asperities can account for adhesion hysteresis. Despite the inherent complexity of the rough gold/mica interface, the adherence properties of this system are sufficiently well characterized to serve as a basis for further studies of model sub-boundary lubricants and their role in adhesion.

In the present study, deformation and adhesion between a self-assembled monolayer (SAM) adsorbed to a microscopically rough gold film in contact with mica in the SFA is considered. Two SAMs are investigated: the methyl-terminated *n*-octadecanethiol (CH₃(CH₂)₁₇SH) and the alcohol-terminated 1-hydroxylunicosanethiol (HO(CH₂)₂₁SH). A contact mechanics approach is used to study the impact of these adsorbed films on adhesion. In particular, changes in the nominal area of contact with load are tracked concurrently with deformations at the interface. Distinct differences between the behavior of bare and coated gold can be ascribed to the presence and performance of these SAMs.

Experimental Method

These contact mechanics studies use a SFA which is identical to ones described in detail elsewhere.^{32,17} This surface forces balance technique works in conjunction with multiple beam interferometry (MBI),¹⁹ and thus the experimental surfaces are part of an interference filter.²⁰ For the case studied here, the experimental surfaces comprise a monomolecular film chemisorbed to rough gold and smooth mica. We describe below the following: (1) details on construction of the interference filters used in this study, (2) a short description on how interference fringes are used to provide information on degree of roughness (as expressed in terms of an equivalent air gap) and associated microdeformations, with particular attention paid to error analysis, and (3) experimental protocol as designed for these studies.

Construction of Interference Filters. The interference filter used in this study includes two thin and uniformly thick mica sheets, cleaved so the surfaces are smooth on a molecular scale. Muscovite mica was cleaved into thin sheets, approximately 3–4 μm, of uniform thickness. Squares of mica (typically 1 cm²) were then cut from this sheet and placed on two large support plates of freshly cleaved mica.

A thin silver film was thermally evaporated onto one of the support plates from a tungsten boat in a turbo-pumped Pyrex bell-jar system, thus covering the exposed faces of the mica sheets. Evaporation rates and final film thicknesses were measured using a quartz crystal monitor. The source metal was 99.999% pure. Base pressure during the evaporation was less than 8 × 10⁻⁷ Torr. Rates of evaporation for silver ranged between 3.5 and 4.0 Å/s. Film thickness was approximately 500 Å. One of the silvered mica sheets was removed and glued to a cylindrical quartz disk by using epoxy resin Epon 1004 (Shell), with the metal side against the resin and the bare mica surface exposed. The disk was then affixed in the SFA on the upper rigid mount.

(17) Israelachvili, J. N.; Adams, G. E. *J. Chem. Soc., Faraday Trans. 1* **1978**, *74*, 975.

(18) Maugis, D.; Barquins, M. J. *J. Phys. D: Appl. Phys.* **1978**, *11*, 1989–2023.

(19) Tolansky, S. *Multiple-Beam Interferometry of Surfaces and Films*; Oxford University Press: London, 1948.

(20) Israelachvili, J. N. *J. Colloid Interface Sci.* **1973**, *44*, 259.

(21) Christenson, H. K. *J. Phys. Chem.* **1993**, *97*, 12034–12041.

(22) Chen, Y. L.; Helm, C. A.; Israelachvili, J. N. *Langmuir* **1991**, *7*, 4–2699.

(23) Chaudhury, M. K.; Whitesides, G. M. *Science* **1992**, *255*, 1230.

(24) Brown, H. R. *Macromolecules* **1993**, *26*, 1666.

(25) de Gennes, P. G. *Langmuir* **1996**, *12*, 4487.

(26) Levins, J. M.; Vanderlick, T. K. *J. Colloid Interface Sci.* **1997**, *185*, 449.

(27) Levins, J. M.; Vanderlick, T. K. *J. Colloid Interface Sci.* **1993**, *158*, 223.

(28) Levins, J. M.; Vanderlick, T. K. *Langmuir* **1994**, *10*, 2389–2394.

(29) Levins, J. M.; Vanderlick, T. K. *J. Phys. Chem.* **1992**, *96*, 10405.

(30) Levins, J. M.; Vanderlick, T. K. *J. Phys. Chem.* **1995**, *99*, 5067–5076.

(31) Quon, R. A.; Knarr, R. F.; Vanderlick, T. K. *J. Phys. Chem. B* **1999**, *103*, 5320–5327.

(32) Vanderlick, T. K.; Scriven, L. E.; Davis, H. T. *Colloids Surf.* **1991**, *52*, 9.

The lower surface was prepared by gluing a bare mica sheet from the other support plate to another cylindrical quartz disk, whereupon the disk was placed in the evaporation chamber and a thin gold film of 500-Å thickness was deposited onto the mica surface. Gold of 99.999% purity was thermally evaporated at a rate of 2.5 Å/s under a base pressure of less than 8×10^{-7} Torr. Our facility allows up to two disks to be coated simultaneously; thus, two gold films are formed under the exact same conditions. This batch preparation allows us to compare the contact mechanics between near identical surfaces, as well as those prepared in separate evaporations. Indeed, despite constancy of evaporation conditions, we have found that surfaces from the same batch behave more similarly than those prepared from different evaporations.³¹

Solutions of octadecanethiol (Aldrich) and 1-hydroxyluniconanethiol (synthesized by A. Ulman, Polytechnic University) are prepared in ethanol through which nitrogen was bubbled. The concentration of each solution is 0.5 mM. The thin gold films prepared above are then placed in one of these solutions under a nitrogen blanket for periods of 6–12 h. SAMs of these alkane-based thiols on gold have been extensively characterized by various surface analytical techniques and theoretical simulations.^{3,4}

After being vigorously rinsed with ethanol and blown dry with a continuous stream of nitrogen, a SAM-modified gold disk was then mounted to the leaf-spring in the SFA, opposite the bare mica surface. Thus, the interference filter has the final form of silver/mica/intervening medium/SAM/gold. The final step prior to experimentation involved sealing the SFA with a small vial of desiccant and then purging with nitrogen gas for at least 0.5 h.

The monolayer formed atop the gold film changes the surface chemistry but leaves the topography of the underlying substrate unchanged. Analysis by our AFM facility shows gold films prepared in the manner above shows our rough surfaces to be well-described as a Gaussian distribution of asperities^{33,14} with a rms roughness of 19 Å and a density of 2600 peaks per μm^2 . The radius of curvature of the asperities is estimated from the rule of thumb of Greenwood and Williamson³⁴ to fall between 60 and 100 Å. These values are consistent with the analysis of other experimenters.³⁰ The presence of a monolayer would increase the radius of curvature by the thickness of the adsorbed film.

Measurement of Microdeformations. The construction of the interference filter for these experiments allows us to directly measure deformations in both the bulk geometry and the interfacial microstructure concurrently.³¹ Interferometric characterization of the rough metal interface is described in detail by Levins et al.^{28,30} We provide below the salient features of this characterization with particular attention to the error analysis.

MBI is very sensitive to the presence of dielectric trapped between the interferometric mirrors. Key to transforming the raw interferometric data into quantitative information related to the structure and degree of surface roughness is to compare the light transmitted through the rough interface to one which is perfectly smooth.^{26,28}

Conversion of this measured shift to an absolute measure of roughness requires a model for the surface topography. For a given model, one varies the extent of roughness until the measured spectrum matches the model spectrum. Different models will yield different measures of roughness, but Levins et al.³⁰ found the extent of variability can be bracketed. Measures of roughness for this study are determined by the “spike” model, where the gold film is determined to be smooth except for a few random protrusions. Thus, the roughness is characterized by a model based on the thickness of a thin uniform layer of gas (termed “equivalent air gap”) trapped between smooth mica and an organic layer (the SAM) which is bound to a smooth gold film.

Relating this absolute measure of nonintimacy to standard definitions of roughness is qualitative at best. Moreover, sources of error in this measure are multiple. The errors reported below are standard deviations from experimental data accumulated

over years of experimentation on similar systems and include upward of 60 different experiments.

First, any accurate measure in the SFA requires alignment of the optical path through the interference filter. This involves making sure light is passed normally through the filter and ensuring that the image of the surfaces is centered on the slit of spectrometer that is used to disperse the interference fringes. Improper normalization will misrepresent the measured roughness. Typically, this alignment procedure is performed while the surfaces are in contact as the filter is presumed to be unchanging. Unfortunately, this procedure cannot be followed strictly in our experiments because asperities deform once contact is initiated. Moreover, our experimental protocol (see below) requires that a load be continuously applied and varied once the bodies contact. Hence, normalization and centering of the white light passed through the filter must be performed before contact is established. These constraints introduce error to absolute measures of roughness, easily 25 Å.

Roughness measurements are dependent on the model chosen, as mentioned above. While the “spike” model provides a good measure of magnitude, the model still imperfectly describes the resultant spectra due to the real character of the metal’s surface roughness. The accuracy of the model depends on the inputs to the model such as optical constants, the mica, and metal thickness, among others. Error in these parameters produces varied measures of roughness. Standard error due to the model range from 2 to 10 Å.

Last, materials composing the interference filter affect the nature of the transmitted spectra. Filters employing gold as one of the reflective films result in spectra generally noisier and broader than ones employing only silver. Spectral deviations measured for gold (0.24 Å in wavelength) are two times that for silver. (In general, wavelength deviations lead to errors in thickness that are approximately an order or magnitude larger.)

Finally, and most importantly, we note that while the accuracy of the measurement is not at angstrom level, the precision of the measurement is. In other words, changes in roughness can be measured with near angstrom level precision and are not sensitive to the topographical model employed.³⁵ In this particular study, it is these changes which are important.

Experimental Protocol. Design of our experiments must consider the dynamics of rough gold deforming against mica in the absence of external loads; surface forces alone act to reduce roughness over time.²⁹ Quon et al. characterized the time dependent nature of this phenomenon for contact between rough gold and mica.³¹ To lessen the effect of this natural relaxation, in the experiments performed here we vary the load quickly and continuously.

Control of the applied force allows us to account for the external load, P , that serves as an independent variable in contact mechanics studies. To this end, a rate of 7.6 μN per second was steadily applied while loading and unloading the surfaces. In what we henceforth refer to as a JKR-style experiment, compressive loads of up to 0.025N were reached before retracting the surfaces back to zero load, whereupon tensile loads were applied until the surfaces jumped apart. The deflection of the spring at the moment of separation is very nearly equal to the separation of the surfaces after the jump, as determined by multiple beam interferometry. The strength of adhesion, or the pull-off force, is simply equal to the deflection of the spring multiplied by the known spring constant. This pull-off force can be related to the work of adhesion as determined by JKR theory.¹²

Results

Pull-off Forces. In the absence of a monolayer coating, and despite a consistent experimental protocol, the pull-off force required to separate gold from mica is highly variable, measuring 347 ± 237 mN/m. Indeed our most significant finding is that the presence of a self-assembled monolayer sharply defines the strength of adhesion as measured by the pull-off force. In particular, after a JKR-style experiment, pull-off forces for contact between octadecanethiol-coated gold and mica measure 159 ± 14

(33) Thomas, T. R. *Rough Surfaces*; Longman Group Limited: Harlow, 1982; p 261.

(34) Greenwood, J. A.; Williamson, J. B. P. *Proc. R. Soc. London, A* **1966**, *290*, 300–319.

(35) Levins, J. M. Ph.D., University of Pennsylvania, 1994.

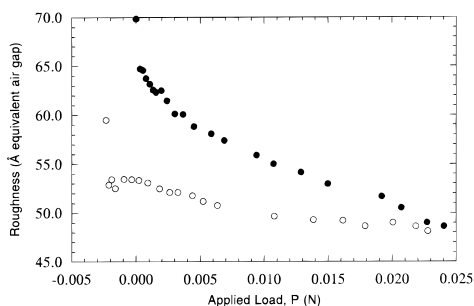


Figure 1. Roughness change with applied load at a rough gold/mica interface. For this system the effective radius of curvature of the interacting bodies, R , is 0.020 m and the effective bulk elastic constant, K , is 25 GPa.

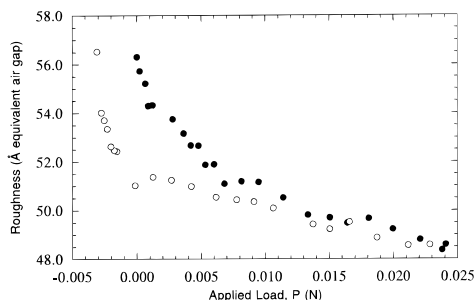


Figure 2. Observed deformations between mica and *n*-octadecanethiol adsorbed on rough gold. For this experiment R is 0.0187 m and K is 17 GPa.

mN/m. Similarly for contact between 1-hydroxylunicosanethiol-coated gold and mica, pull-off forces measure 371 ± 65 mN/m.

Micromechanical Deformations. The effect of the monolayers on mechanical deformations at the interface is best understood in relation to deformations of an uncoated gold film against mica. Detailed studies performed by us and others find gold asperities deform plastically under the action of surface forces and applied loads.^{30,31,35} After initial contact, deformations totaling 23 ± 7 Å are measured during JKR-style experiments for loading up to 0.025 mN (based on four sets of experiments). Moreover, in a typical contact experiment, little recovery of the deformation is observed until just prior to separation, as illustrated in Figure 1; sometimes, no recovery of the deformation is observed.

Presence of the self-assembled monolayer changes the microdeformation behavior in two distinct ways. One is to limit the extent of asperity deformations. For instance, upon compression to the same total load, the change in measured roughness of octadecanethiol-coated gold against mica is 10 ± 3 Å. For 1-hydroxylunicosanethiol-coated gold pressed against mica it is 15 ± 7 Å (based on four sets of experiments for each SAM).

The presence of the SAM also results in an immediate and reversible recovery of deformations upon relief of the applied load, as shown in Figure 2. We observe, for both SAMs, an elastic recovery in the microdeformation behavior upon retracting the load. This reversibility is limited to 4.4 ± 0.9 Å of recovery, at which point, the loading and unloading behavior diverge. The possibility that this region of elastic behavior results from a relaxation and stretching of the monolayer is examined in the Discussion.

Bulk Deformations and Adhesion Hysteresis. Deformation of asperities at the interface is accompanied by deformations of the bulk geometry, as captured by the shape of the interference fringes. Since contact between

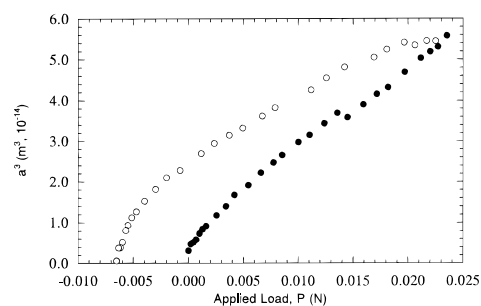


Figure 3. Loading (filled circles) and unloading (empty circles) behavior of the contact diameter for mica against gold coated with 1-hydroxylunicosanethiol. R is 0.0189 m and K is 20 GPa.

crossed cylinders is similar to contact between a sphere and a flat plate, the flattened region of the fringes reasonably estimates the diameter of a circular contact region. Monitoring the changes of this contact diameter with applied loads permits us to relate our observations to the JKR theory of contact mechanics and in particular to compare the behavior of SAM-coated gold to that of bare gold as previously studied.³¹

As with bare gold, the bulk deforms in a hysteretic fashion with applied load, as show in Figure 3; unloading results in greater contact areas than the corresponding loading process. Such hysteresis is, of course, not accounted for in JKR theory. However, by using JKR theory as an interpretive tool we could demonstrate, for the case of bare gold against mica, a correlation between bulk deformations and microdeformations. The bulk deformed in a manner whereby the effective adhesion strength increased with increasing loads, concurrent with deformations of the asperities; the effective adhesion strength decreased upon release of the stress in a commensurate fashion with any recovery of the asperity deformation.³¹ We saw no such correlation for the SAM-coated gold. This is most evident by simply considering the point of load reversal: the microdeformations are reversible while the bulk deformations are clearly not (the nominal area of contact hardly changes). In other words, although the effective roughness is increasing upon retraction, the effective adhesion strength of SAM-coated gold to mica does not exhibit a commensurate decrease. The presence of the monolayer is somehow responsible for maintaining an increased effective strength of adhesion. We also note that the degree of hysteresis was larger for the alcohol-terminated monolayer than for the methyl-terminated monolayer.

Discussion

Clearly SAMs offer control over surface chemistry and thus on surface energetics which directly influence adhesive strength. The force required to pull the hydrophilic mica apart from the alcohol-terminated coating is about twice as large as that for the methyl-terminated coating. However, equally, if not more, valuable is the ability of such coatings to precisely define and maintain their respective surface energies, especially relative to that for the uncoated gold surface. The variation of adhesion measurements is much narrower for coated gold: variation, as a percentage of the measured adhesion, is reduced by a factor of 4 for the octadecanethiol monolayer and by a factor of 8 for the 1-hydroxylunicosanethiol monolayer.

These monomolecular films not only modify surface chemical properties but influence surface mechanical properties as well. Compared to the behavior of uncoated gold, microdeformations are reduced in absolute magni-

tude upon loading to the same degree. Moreover they exhibit a regime of reversible behavior about the point of maximum load; in contrast, the state of deformation at the bare gold/mica junction remains fixed for significant duration when the load is reversed.

One might conjecture that the reduced amount of microdeformation in the case of the octadecanethiol monolayer may result from the fact that lesser surface energies act to bring the surfaces closer together. Measured pull-off forces between 1-hydroxylunicosanethiol-coated gold and mica are, however, slightly higher than the comparable bare gold/mica system. In view of the latter, the lesser amount of microdeformation measured for this system clearly does not result from any difference in surface energetics. It thus appears that the mere presence of the SAM serves to strengthen the underlying gold asperities and thus restricts their degree of deformation. This apparent resistance to deformation may likely arise from energetically unfavorable rearrangements of the SAM molecules as caused by deformations of the asperities beneath them.

A unique characteristic of the microdeformation behavior of coated gold, seen for both SAMs, is the recovery of deformation upon load reversal. As we see no such behavior with uncoated gold, we believe that this particular phenomenon is associated with compression of the self-assembled monolayer. Monte Carlo simulation of *n*-hexadecanethiol monolayers under mechanical compression also shows a near-elastic relaxation upon removal of applied stress.³⁶ These simulations suggest a monolayer may be compressed to approximately 75% of its initial thickness; higher loads are likely to result in damage to the monolayer. Loss of thickness is associated with changes in tilt angle as well as generation of defects within the monolayer itself.³⁶

Joyce et al.³⁷ used interfacial force microscopy to study the compression between a tungsten tip and *n*-hexadecanethiol monolayer atop gold. They found that the film could be compressed to about 20% of its initial value. Compression of the monolayer beyond the moderate load range identified by Siepmann et al.³⁶ resulted in an indentation of the underlying substrate. In addition, large adhesion hysteresis was observed upon relief of the stress. This behavior suggests very substantial rearrangement within their monolayer, perhaps to the point of its destruction. As our experiments show no hysteresis at the interface upon relief of the stress, and the observed elastic relaxation corresponds to a compression of only 80% of the initial thickness the SAM, our adsorbed monolayers likely maintain their integrity.

Our measured response of microdeformations to loading, such as that shown in Figure 2, can be recast in terms of stress/strain data so as to provide estimates of the SAM compressibilities. Since the pressure distribution under the contact region is not uniform, we followed the strategy of Chen et al.²² who used JKR to estimate the stress at the center of the contact zone:

$$\sigma = \frac{1.5P + 3\pi WR + [6\pi WRP + (3\pi WR)^2]^{1/2}}{\pi a^2}$$

Note, calculation of this stress requires a measure of *W*. This interfacial energy, however, varies with the degree

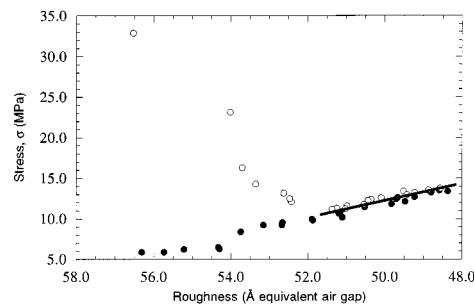


Figure 4. Roughness as a function of applied stress for *n*-octadecanethiol adsorbed on gold and pressed against mica. The solid line identifies the region assumed to result from the elastic compression and relaxation of the monolayer. Estimation of the compressibility of the bound monolayer, K_M , is 25 MPa, where R is 0.0162 cm and K is 11 GPa.

of roughness.³¹ Therefore, to determine the stress, the approach of Quon et al.³¹ is used to account for changes in *W*.

We can use the resultant strain/stress data, such as that shown in Figure 4, to estimate the compressibility of the SAMs used in this study. We first make due note of the fact that the total deformation we measure via interferometry arises from the sum of deformations of all components making up the optical filter. This filter includes a piece of mica several micrometers thick, the silver and bulk gold films which serve as mirrors to generate multiple reflections, the SAM layer, and the "effective air gap". The mica and metal layers are the most incompressible, but they are the thickest and so their respective deformations cannot necessarily be ignored. Fortunately, the thickness of the bulk metal has little effect on the wavelengths of the transmitted interference fringes, hence deformations of the bulk gold and silver are not responsible for the wavelength shifts observed. The deformation of the mica sheet is estimated to be no more than few angstroms for the forces applied in this study. On the other hand, in the case of uncoated gold, the elastic response of the mica was not observed, i.e., reversal of load is accompanied by no change in deformation. Hence we shall take no account of mica thickness change in these experiments with the caveat that this would lead to underestimation of the SAM compressibility. The more significant assumption is that the elastic deformation observed upon load reversal is solely attributed to the monolayer and not partly to deformations of the underlying asperities. Again, since we see no such elastic deformations in the absence of the SAM,³¹ we proceed with this notion.

Monolayer compressibility, K_M , is then determined by the slope of the region on the stress/strain plot in which elastic behavior is noted:

$$K_M = \frac{\Delta\sigma}{\Delta D/D}$$

where σ is applied stress at the center of contact region (discussed above) and D is the thickness of the monolayer. Following this procedure we find the compressibility of octadecanethiol monolayer to be 26 ± 2 MPa, while that of 1-hydroxylunicosanethiol is 40 ± 15 MPa.

These results can be compared to other measurements on related systems. Chen et al.²² reported compressibility values of DMPE monolayers in different phase states; the compressibility of crystalline condensed monolayers measured 178 MPa, while crystalline expanded monolayers measured 56 MPa for a coverage of $67 \text{ \AA}^2/\text{molecule}$. Our determinations are lower than those of Chen et al.,²² but on the same order of magnitude. Even if half of our

(36) Siepmann, J. I.; McDonald, I. R. *Phys. Rev. Lett.* **1993**, *70*, 453–456.

(37) Joyce, S. A.; Thomas, R. C.; Houston, J. E.; Michalske, T. A.; Crooks, R. M. *Phys. Rev. Lett.* **1992**, *68*, 2790–2793.

observed deformation is attributed to changes in mica or gold, the order of magnitude remains the same, and the measured values would be more in keeping with those measured by Chen et al.²² The difference may also be due to structural differences in the monolayer; the phospholipid DMPE is double tailed, in contrast to the single-chained alkylthiols, which may add more rigidity in the structure. Note, in the same study by Chen et al.,²² the compressibility of CTAB, a single chained molecule, measured 51 MPa. Second, and more importantly, the underlying roughness may effectively add conformational degrees of freedom. While SAMs are known to form a well-packed, crystalline monolayer, their packing may be more open on the edges and crowns of asperities in contact with the mica. Moreover, the SAM may not be as well-packed as one might assume since no procedure to anneal the monolayer was followed.^{38–41} (Annealing the SAMs by heating the substrate affects the gold film morphology by changing the underlying roughness. Consequently, comparisons between various SAM-coated gold films and uncoated gold films could not be made with any degree of confidence; control of the roughness statistics for the underlying gold would be lost.)

In addition to having an effect on the microdeformations, the presence of the monolayer also had an effect on the bulk deformation behavior. In particular, a hysteresis in contact area is observed that cannot be correlated with a hysteresis in microdeformation behavior as we have previously observed for bare gold in contact with mica. One mechanism accounting for the hysteresis of the bulk deformation may lie in the monolayer's ability to stretch as loads are relieved. In effect, the nominal contact area may reduce more slowly as the surfaces retreat because the SAM is able to "grip" the opposing surface more effectively than a rigid gold film. A tensile reorientation of the monolayer is suggested by Burns et al.⁴⁰ who studied friction between a glass tip and an alkanethiol monolayer using a novel scanning probe microscope. Unfortunately, the force microscopy approach cannot directly verify this reorientation, but this complementary technique does note that adhesion hysteresis was dependent on the chemical

functionality of the lubricant. In particular, stronger frictional and adhesive forces were noted for 1-carboxylundecanethiol monolayers versus *n*-dodecanethiol.⁴⁰ Likewise, we also find that hysteretic behavior is qualitatively greater for contact between 1-hydroxylundecanethiol and mica than for the other less adherent SAM.

Last, we note that as unloading proceeds the SAM-coated gold exhibits a sharp recovery of asperity deformation just prior to separation. Seemingly, when the monolayer is unable to accommodate the tensile stress, the underlying substrate then plastically deforms until sufficient tension exists to separate the surfaces. This behavior is also observed during contact mechanics studies between gold and mica.³¹

Conclusions

The chemisorption of a SAM upon gold modifies both the chemical and mechanical surface properties. Control over the strength of adhesion becomes well-defined and precise. Over the load ranges studied, elastic behavior at the interface is noted and is attributed to the mechanical properties of the SAM. Assuming the deformations result solely from changes to the SAM, compressibilities of the monolayers can be determined. The values are on the same order as those for Langmuir–Blodgett films measured by other investigators.²²

The reversible nature of microdeformations observed at the interface is not reflected in the associated bulk deformations. In other words, the bulk deformations observed upon unloading the SAM-coated gold from the opposing mica sheet are unexplainably high. This macroscopic manifestation of an increased adhesion may arise from a tensile reorientation of the monolayer.

Last we believe this work demonstrates the promise of the SFA for studying the role of sub-boundary lubricants on adhesion. The apparatus is also well-suited for investigating the effects of humidity and other environmental changes on this phenomenon. The power of this approach lies in the ability to directly observe changes in microstructure at the interface with concurrent changes over a macroscopic contact region. Further study of adhesion and lubrication on these microscopic dimensions is critical as technology moves to ever finer scales.

Acknowledgment. We gratefully acknowledge support for this work from the National Science Foundation (CTS-9615868).

LA990694T

(38) Delamarche, E.; Michel, B.; Gerber, C.; Anselmetti, D.; Güntherodt, H.-J.; Wolf, H.; Ringsdorf, H. *Langmuir* **1994**, *10*, 2869–2871.

(39) Delamarche, E.; Michel, B.; Kang, H.; Gerber, C. *Langmuir* **1994**, *10*, 4103–4108.

(40) Burns, A. R.; Houston, J. E.; Carpick, R. W.; Michalske, T. A. *Langmuir* **1999**, *15*, 2922–2930.

(41) Schonenberger, C.; Jorritsma, J.; Sondag-Huethorst, J. A. M.; Fokkink, L. G. J. *J. Phys. Chem.* **1995**, *99*, 3259–3271.